Holstein Polarons Near Surfaces

Glen L. Goodvin, Lucian Covaci, and Mona Berciu

Department of Physics and Astronomy, University of British Columbia, Vancouver, British Columbia, Canada V6T 1Z1

(Received 7 June 2009; published 22 October 2009)

We study the effects of a nearby surface on the spectral weight of a Holstein polaron, using the inhomogeneous momentum average approximation which is accurate over the entire range of electron-phonon (e-ph) coupling strengths. The broken translational symmetry is taken into account exactly. We find that the e-ph coupling gives rise to a large additional surface potential, with strong retardation effects, which may bind surface states even when they are not normally expected. The surface, therefore, has a significant effect and bulk properties are recovered only very far away from it. These results demonstrate that interpretation in terms of bulk quantities of spectroscopic data sensitive only to a few surface layers is not always appropriate.

DOI: 10.1103/PhysRevLett.103.176402 PACS numbers: 71.38.−k, 63.20.kd, 72.10.Di

Understanding the behavior of a particle coupled to bosons from its environment (phonons, magnons, etc.), is a problem relevant for many interesting materials: manganites, cuprates, most other oxides, organic materials, cold atoms, etc. A well-known result is the formation of a polaron—the particle is dressed by a phonon cloud. Although this is an old problem [1], there is still considerable analytical and numerical effort being made towards understanding simple Hamiltonians, like the Holstein model [2,3]. Most of this work has been focused on calculating bulk properties. However, many materials are being investigated nowadays using surface-sensitive spectroscopies, such as scanning tunneling microscopy (STM) [4] and angle-resolved photoemission spectroscopy (ARPES) [5]. Although the former probes only the surface layer while the latter probes the first few layers, they are usually interpreted in terms of bulk densities of states or spectral weights.

In this Letter we show that the properties of polarons near surfaces are significantly different from bulk behavior. Our results demonstrate that interpretation of data from surface spectroscopies in terms of bulk quantities is generally not warranted. These results are also relevant for the very active area of oxide-based nanostructures, where remarkable behavior, e.g., superconductivity, is seen at the interface between two insulators [6]. While strong correlations (not addressed at this single-polaron level) are obviously important, in most oxides the charge carriers also couple strongly to phonons, magnons and/or orbitons. Our demonstration that such coupling gives rise to significant additional potentials near the interface is clearly important for properly understanding these systems.

Here we introduce a method that allows for efficient yet accurate investigation of such problems, and which we expect to become a basic tool for interpretation of experimental data of systems where polaronic effects are important. This method—the inhomogeneous momentum average (IMA) approximation —is based on the momentum average (MA) approximations used to study bulk properties of Holstein [7] and more complex polaron models [8]. MA was shown to be highly accurate over all parameter space, in all dimension and at all energies, for all of these models. Here we use the Holstein model to illustrate the new phenomenology; the quantitative changes expected for the more general models can be studied similarly.

The IMA method was recently developed to investigate the effects of disorder on polaron properties [9]. Comparison with exact but expensive diagrammatic Monte Carlo simulations [10] proved that the high accuracy is maintained for problems with broken translational symmetry. This is expected since IMA makes no further approximations to MA, so it is based on the same physical arguments as MA and satisfies the same number of spectral weight sum rules, exact asymptotic limits, etc. [7].

Here we extend IMA to study systems with surfaces. For simplicity, we consider crystal-vacuum interfaces and forbid the wave functions from spilling into the vacuum. This approximation, which implies an infinite work function, can be easily relaxed. In fact, with this method we can also study interfaces between two materials with different band structures, boson frequencies and particle-boson couplings. To show the versatility of the method we add a surface potential, whose value controls the tendency to bind surface states. We take this potential to be uniform on the surface, so as to not break in-plane translational invariance. However, localized impurity potentials can also be added and treated as discussed in Ref. [9], allowing, e.g., for realistic modeling of STM spectra in the vicinity of various impurities. Since we treat these terms exactly, we expect the accuracy to remain as high as for all other MA-based results. To our knowledge, these are the first available results for such problems [11].

We calculate the polaron Green's functions $G(i, j, \omega) = \langle 0|c_i \hat{G}(\omega) c_j^\dagger|0\rangle = \sum_\alpha \langle 0|c_i|\alpha\rangle\langle\alpha|c_j^\dagger|0\rangle/(\omega - E_\alpha + i\eta)$, where $\hat{G}(\omega) = [\omega - \mathcal{H} + i\eta]^{-1}$, $\mathcal{H}$ is the Hamiltonian and c_i the electron annihilation operator at site i. The spin of the electron is irrelevant, and we set $\hbar = 1$. As usual, the

poles mark the single-polaron spectrum $\hat{\mathcal{H}}|\alpha\rangle = E_\alpha|\alpha\rangle$. The spectral weight (measured by ARPES) and local density of states (measured by STM) are obtained from the Green's function in the usual way [4,5].

We first review the exact Green's function of the system with a surface, in the absence of e-ph coupling [12]. We solve the problem for a semi-infinite one-dimensional (1D) chain and then generalize. For an infinite chain with periodic boundary conditions and nearest-neighbor (nn) hopping $\hat{\mathcal{H}}_0 = -t\sum_i (c_i^\dagger c_{i+1} + \text{H.c.})$, we have

$$G_0(i, j, \omega) = \frac{1}{2\pi}\int_{-\pi}^{\pi} dk \frac{e^{ik(R_i - R_j)}}{\omega - \varepsilon_k + i\eta}, \qquad (1)$$

where $\varepsilon_k = -2t\cos k$ since we take the lattice constant to be $a = 1$. Other dispersions can be treated similarly.

To calculate the Green's function $G_c(i, j, \omega)$ for a semi-infinite chain that starts at site 0, we "cut" the infinite chain by adding $\hat{V}_{\text{cut}} = +t(c_{-1}^\dagger c_0 + c_0^\dagger c_{-1})$, so that $\hat{\mathcal{H}}_c = \hat{\mathcal{H}}_0 + \hat{V}_{\text{cut}}$ has no hopping to the left from site 0. Applying Dyson's identity $\hat{G}_c(\omega) = \hat{G}_0(\omega) + \hat{G}_0(\omega)\hat{V}_{\text{cut}}\hat{G}_c(\omega)$ we find that for any $i,\ j \geq 0$, $G_c(i, j, \omega) = G_0(i, j, \omega) + tG_0(i, -1, \omega)G_c(0, j, \omega)$, which is solved to give

$$G_c(i, j, \omega) = G_0(i, j, \omega) + t\frac{G_0(i, -1, \omega)G_0(0, j, \omega)}{1 - tG_0(0, -1, \omega)}. \qquad (2)$$

If the energy of site 0 is also modulated by a surface potential $\hat{U}_0 = -Uc_0^\dagger c_0$, the total Hamiltonian of the chain is $\hat{\mathcal{H}}_s = \hat{\mathcal{H}}_c + \hat{U}_0$ and its Green's function is calculated by applying Dyson's identity again, leading to:

$$G_s(i, j, \omega) = G_c(i, j, \omega) - U\frac{G_c(i, 0, \omega)G_c(0, j, \omega)}{1 + UG_c(0, 0, \omega)}. \qquad (3)$$

$G_s(i, j, \omega)$ can be calculated similarly for any other surface potential, including modulated hopping terms.

To generalize, we consider a d-dimensional simple cubic crystal with nn hopping and a (100) surface (any other surface can be treated similarly [12,13]). Because of the symmetry to in-plane translations, we partially Fourier transform and use operators $c_{i,\mathbf{k}}$ which annihilate a particle with in-plane momentum $\mathbf{k}$ from the layer $i \geq 0$. Then $\langle 0|c_{i,\mathbf{k}'}\hat{G}_s(\omega)c_{j,\mathbf{k}}^\dagger|0\rangle = \delta_{\mathbf{k},\mathbf{k}'}G_s(\mathbf{k}, i, j, \omega)$ because $\mathbf{k}$ is a good quantum number. Moreover, the Hamiltonian factorizes into a sum of 1D problems, one for each $\mathbf{k}$, so that $G_s(\mathbf{k}, i, j, \omega) = G_s(i, j, \omega - \varepsilon_{\|,\mathbf{k}})$ where $G_s(i, j, \omega)$ is the 1D solution of Eq. (3) and $\varepsilon_{\|,\mathbf{k}} = -2t\sum_{i=1}^{d-1}\cos k_i$ is the kinetic energy for the in-plane motion. Given the distinction between where the in-plane hopping $t_\|$ appears (in $\varepsilon_{\|,\mathbf{k}}$) and where the interlayer hopping $t_\perp$ appears [in Eqs. (1) and (2), defining the 1D functions G_0 and G_c], it is trivial to generalize to anisotropic hopping. A full analysis for $t_\perp \neq t_\|$ will appear elsewhere [13], but we note that for intermediate values of the e-ph coupling, the surface effects discussed here are significant if $t_\perp/t_\| \gtrsim 0.1$.

Finally, note that (100) surfaces do not bind surface states if $U = 0$, when $G_s = G_c$ of Eq. (2) has no poles outside the continuum. Such poles appear for a large enough surface attraction $U \geq t$, when Tamm surface states form [14]. This is true in all dimensions.

Now we add the e-ph coupling to our d-dimensional system with the (100) surface, described by $\hat{\mathcal{H}} = \hat{\mathcal{H}}_s + \hat{\mathcal{H}}_{\text{ph}} + \hat{V}_{e\text{-ph}}$, where $\hat{\mathcal{H}}_s$ has been discussed, $\hat{\mathcal{H}}_{\text{ph}} = \Omega\sum_{i\geq 0,\mathbf{q}} b_{i,\mathbf{q}}^\dagger b_{i,\mathbf{q}}$ describes a branch of Einstein optical phonons of energy Ω, where $b_{i,\mathbf{q}}^\dagger$ creates a boson with in-plane momentum $\mathbf{q}$ in the layer i, and

$$\hat{V}_{e\text{-ph}} = \frac{g}{\sqrt{N_\|}}\sum_{i\geq 0}\sum_{\mathbf{k},\mathbf{q}} c_{i,\mathbf{k}-\mathbf{q}}^\dagger c_{i,\mathbf{k}}(b_{i,\mathbf{q}}^\dagger + b_{i,-\mathbf{q}})$$

is the Holstein coupling. $N_\| \to \infty$ is the number of unit cells in the surface edge (if $d = 2$), or the surface layer (if $d = 3$), and the $\mathbf{k}$, $\mathbf{q}$ sums are over the in-plane Brillouin zone (BZ). For a chain ($d = 1$), they do not appear.

Using the exact Green's function $G_s(\mathbf{k}, i, j, \omega)$ for the noninteracting part of $\mathcal{H}$, we can map this problem onto that discussed in Ref. [9], with G_s replacing the disorder Green's function G_d appearing there. Then the IMA approximations are obtained quite similarly; we summarize here the main results. Since $\mathcal{H}$ is invariant to in-plane translations, it only has finite matrix elements between states with the same in-plane momentum:

$$\langle 0|c_{i,\mathbf{k}}\hat{G}(\omega)c_{j,\mathbf{k}'}^\dagger|0\rangle = \delta_{\mathbf{k},\mathbf{k}'}G(\mathbf{k}, i, j, \omega).$$

Both $n = 0$ and 1 IMA$^{(n)}$ approximations lead to implicit solutions for $G(\mathbf{k}, i, j, \omega)$ with the same formal structure:

$$G_{\text{IMA}^{(n)}}(\mathbf{k}, i, j, \omega) = G_s(\mathbf{k}, i, j, \tilde{\omega}_n) + \sum_{j'\geq 0} G_{\text{IMA}^{(n)}}(\mathbf{k}, i, j', \omega) \times v_n(j', \omega)G_s(\mathbf{k}, j', j, \tilde{\omega}_n) \qquad (4)$$

where $\tilde{\omega}_n = \omega - \Sigma_{\text{MA}^{(n)}}(\omega)$ is the energy renormalized by the *bulk* polaron self-energy $\Sigma_{\text{MA}^{(n)}}(\omega)$ (see below), and:

$$v_n(j, \omega) = \Sigma_{\text{IMA}^{(n)}}(j, \omega) - \Sigma_{\text{MA}^{(n)}}(\omega) \qquad (5)$$

where $\Sigma_{\text{IMA}^{(n)}}(j, \omega)$ are layer-dependent "self-energies". In particular, $\Sigma_{\text{IMA}^{(0)}}(j, \omega) = gA_1(j, \omega)$ where

$$A_n(j, \omega) = \frac{ng\bar{G}_s(j, j, \omega - n\Omega)}{1 - g\bar{G}_s(j, j, \omega - n\Omega)A_{n+1}(j, \omega)} \qquad (6)$$

are continued fractions defined in terms of *in-plane* momentum averages of the noninteracting Green's functions in that layer: $\bar{G}_s(j, j, \omega) = \frac{1}{N_\|}\sum_{\mathbf{q}} G_s(\mathbf{q}, j, j, \omega)$. For $j \to \infty$, $G_s(\mathbf{q}, j, j, \omega) \to G_0(\mathbf{q}, j, j, \omega)$ as bulk behavior is recovered far from the surface. From Eq. (1) it then follows that $\lim_{j\to\infty}\bar{G}_s(j, j, \omega)$ are the *fully* momentum-averaged free propagators, and thus $\Sigma_{\text{MA}^{(0)}}(j \to \infty, \omega) = \Sigma_{\text{MA}^{(0)}}(\omega)$, the expected bulk MA$^{(0)}$ self-energy [8].

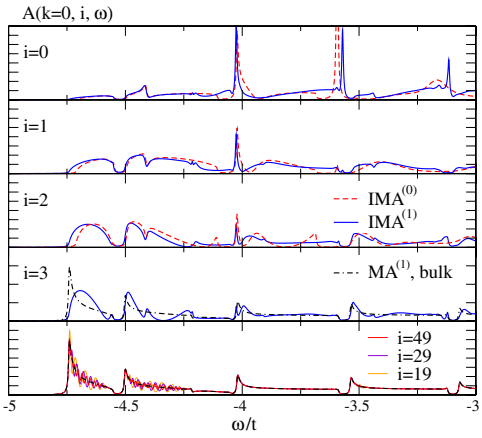

FIG. 1 (color online). $A(k = 0, i, \omega)$ vs ω/t in various layers, for $\Omega = 0.5t$, $g = \sqrt{2}t$, $U = 0$, $\eta = 0.004t$.

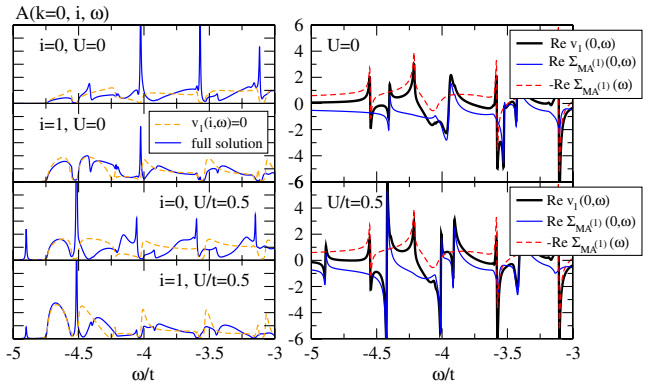

FIG. 2 (color online). Left: Comparison between full $\mathrm{MA}^{(1)}$ solution (solid line) and solution if $v_1(j, \omega) = 0$ (dashed line). Right: Real part of the surface potential $v_1(i = 0, \omega)$ in units of t vs energy. The upper panels are for $U/t = 0$ and the lower are $U/t = 0.5$, while $\Omega = 0.5t$, $g = \sqrt{2}t$, $\eta = 0.004t$.

At the $\mathrm{IMA}^{(1)}$ level, we find $\Sigma_{\mathrm{IMA}^{(1)}}(j, \omega) = g^2 \bar{x}_j(\omega)[1 - g^2 \bar{x}_j(\omega)\{A_2(j, \omega) - A_1(j, \omega - \Omega)\}]^{-1}$, with $\bar{x}_j(\omega) = \frac{1}{N_\parallel}\sum_{\mathbf{q}} G_{\mathrm{IMA}^{(0)}}(\mathbf{q}, j, j, \omega - \Omega)$ the in-plane momentum average of the $\mathrm{IMA}^{(0)}$ solution at a reduced energy [9,13]. This is a more complicated but more accurate expression, since the accuracy of $\mathrm{IMA}^{(n)}$ improves with increasing n [9]. It is straightforward to verify that $\Sigma_{\mathrm{IMA}^{(1)}}(j \to \infty, \omega) = \Sigma_{\mathrm{MA}^{(1)}}(\omega)$, the $\mathrm{MA}^{(1)}$ bulk self-energy [8]. Thus, from Eq. (5) it follows that $v_n(j, \omega)|_{j\to\infty} \to 0$ for both $n = 0$, 1, so this is a surface-related energy.

The first term in Eq. (4) would be the expected solution if the only effect of the e-ph coupling is the formation of the polaron. Then, we could start with the bulk polaron Green's function instead of G_0 in Eq. (1). For MA with $n = 0$, 1, this means renormalizing the energy $\omega \to \omega - \Sigma_{\mathrm{MA}^{(n)}}(\omega) = \tilde{\omega}_n$. Using the same steps to "cut" the surface leads to the first term in Eq. (4). The second term shows that there is more. Its form suggests a Dyson identity coming from adding an extra surface potential $\sum_{j,\mathbf{k}} v_n(j, \omega) c^\dagger_{j,\mathbf{k}} c_{j,\mathbf{k}}$ to the Hamiltonian. Since this potential depends on energy, it encodes the retardation effects due to the surface. In other words, not only the electron, but also the surface potential that it experiences, are renormalized due to the e-ph coupling. As we show now, this additional retarded surface potential is considerable and has very important consequences.

Equation (4) is easy to solve since $v_n(j, \omega)$ vanishes rapidly away from the surface ($j' \leq 5$ cutoffs suffice), and we find any $G(\mathbf{k}, i, j, \omega)$ by solving a few coupled equations. Figure 1 shows $A(\mathbf{k}, i, \omega) = -\frac{1}{\pi}\mathrm{Im}G(\mathbf{k}, i, i, \omega)$ at $\mathbf{k} = 0$, i.e., the spectral weight measured by inverse ARPES if an electron with in-plane momentum $\mathbf{k}$ is injected in layer i. Because of particle-hole symmetry, the ARPES signal for removing an electron from a full band is obtained by inverting $\omega \to -\omega$. These results are for $d = 2$ (the in-plane momentum is a scalar k). We note that we get similar results in any dimension. The top four panels are for $i = 0$, 1, 2, 3, while the fifth shows the convergence towards bulk. The bulk result (dash-dotted line) consists of the polaron band from about $-4.7t$ to $-4.55t$, with a finite width due to integration over the out-of-plane momentum. This is followed by the second bound state, present for this intermediate coupling, then the polaron + one-phonon continuum starting just above it, at around $-4.2t$, and higher energy features [7].

Both $\mathrm{IMA}^{(0)}$ (dashed line) and $\mathrm{IMA}^{(1)}$ (solid line) results are plotted for the first 3 layers. They agree well, proving that there is no need to go to higher IMA levels. However, they are very different from the bulk. Especially for $i = 0$ there is very little weight in the polaron band. As i increases this feature starts to recover towards its bulk value, but full convergence is not reached even at $i = 50$. Higher energy features converge much faster, being quite similar to bulk even for $i = 2$. The weight missing from the polaron band, for $i = 0$, appears as two sharp peaks near $\omega/t \approx -4$ and -3.5, whose heights decrease exponentially as i increases. These are surface states, located in small gaps in the bulk spectrum. Their appearance is due to the additional surface potential, as proved in the left panels of Fig. 2, where we plot for $i = 0$, 1 the full $\mathrm{IMA}^{(1)}$ solution (solid line) and the solution if $v_1(j, \omega) = 0$ (dashed line). The latter has no such surface states.

The location of the surface states depends on the value of U. The lower left panels of Fig. 2 show that for a small $U/t = 0.5$, surface states appear below the polaron band and in the first gap. Again, neither is seen if $v_1(j, \omega) = 0$, in agreement with the fact that a potential $U < t$ alone cannot bind a surface state. (In fact the relevant ratio is U/t^*, where t^* is the effective polaron hopping. For values used in Fig. 2, $U < t^*$.) Apart from the surface states, which are the most visible features, the spectral weights for $U = 0$ and $U/t = 0.5$ are fairly similar (the vertical scale is the same in all panels). For $i \gg 1$ both converge to the same bulk value, shown in Fig. 1.

To understand this behavior we now analyze $v_1(i, \omega)$. We plot its real part for $i = 0$ as a thick solid line in the

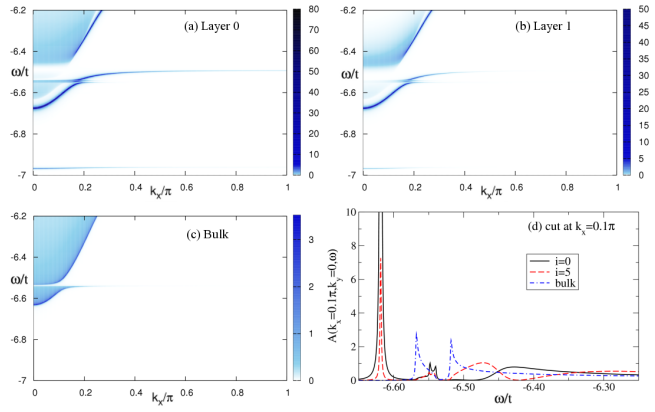

FIG. 3 (color online). 3D spectral weight $A(k_x, k_y = 0, i, \omega)$ vs k_x and ω, for (a) $i = 0$, (b) $i = 1$, and (c) bulk. Note the very different scales for these panels. (d) Cut at $k_x = 0.1\pi$. Parameters are $U = t$, $\Omega = 0.5t$, $g = \sqrt{3}t$, $\eta = 0.001t$.

right panels of Fig. 2, for $U/t = 0$, 0.5. We also plot the layer's self-energy (thin line) and minus the bulk self-energy (dashed line), since $v_1(i, \omega)$ equals their sum, Eq. (5). Consider first the bulk self-energy: it diverges at the top of the polaron band (smoothed by the finite η), where it changes sign and then diverges again at the top of the second bound state band, followed by more complicated behavior in the continuum and at higher energies. Now, $\Sigma_{\mathrm{IMA}^{(1)}}(i, \omega)$ has a similar continued-fraction expression like $\Sigma_{\mathrm{MA}^{(1)}}(\omega)$, see Eq. (6). For $U = 0$, $\bar{G}_s(0, 0, \omega)$ is smaller than the bulk value, since a low-energy free electron is unlikely to be found near such a surface. This is roughly as if we had the bulk value for $\bar{G}_s$ but at a smaller g in Eq. (6), and results in a shift towards higher energies (like a bulk self-energy at a smaller g). This explains why v_1 alternates between large positive and negative values. For $U = 0.5t$, the free electron is more likely to be near the surface, so we see a shift of the $\Sigma_{\mathrm{IMA}^{(1)}}(i, \omega)$ features to lower values than for the bulk, and a v_1 with a different pattern of large positive and negative values. Whenever v_1 is strongly attractive, surface states may appear.

The physical meaning of this retarded surface potential is now clear [9]. The bulk self-energy accounts for the phonon cloud and its binding to the electron. Near the surface, the motion of the electron and its cloud is modified, changing the energetics. This is described by the additional surface potential $v_n(j, \omega)$ we uncovered here, which has to depend nontrivially on ω, since it matters whether the electron's dynamics are coherent or not, etc.

Because of this additional surface potential generated by the e-ph coupling, surface states may appear (and be the dominant spectral features for surface layers) where not otherwise expected. If they are taken to be bulk features, one will extract the wrong parameters from data fits. This is illustrated in Figs. 3(a) and 3(b), where we show the spectral weight in layers $i = 0$, 1 of a (100) surface of a 3D crystal, for in-plane momentum $k_x \in (0, \pi)$, $k_y = 0$. The bulk spectral weight, shown in Fig. 3(c), has a narrow polaron band, and the second bound state band above it (partially shown). Near the surface, the spectral weight in these bands is significantly depleted. The dominant feature is a surface state that lies just under these bands [also see Fig. 3(d)], except where it flattens out, above the gap between the two bulk bands [15]. Given how strong it is, if one tries to fit it to bulk behavior, one may take it to be the signature of a large polaron, with a large quasiparticle weight and significant dispersion. The "break" in dispersion would be taken to signal the continuum expected at "Ω". The flat, low weight surface state seen just above $\omega = -7t$, which in reality indicates how strong the enhanced surface potential is, may be lost in the background noise or attributed to impurities. Such analysis produces wrong estimates for all parameters.

To conclude, we have shown that electron-boson interactions give rise to an additional, strongly retarded surface potential, which changes significantly the polaron behavior near surfaces. Analysis in terms of bulk properties of STM or ARPES data of materials with strong polaronic effects is therefore generally inappropriate.

We thank Antoine Kahn for suggesting this problem to us, and George Sawatzky and Andrea Damascelli for many useful discussions. This work was supported by NSERC, CIfAR, Killam Trusts (G. G.) and KITP through NSF Grant No. PHY05-51164 (M. B.).

[1] L. D. Landau, Phys. Z. Sowjetunion **3**, 644 (1933).
[2] T. Holstein, Ann. Phys. (N.Y.) **8**, 325 (1959).
[3] For a review, see H. Fehske and S. A. Trugman, in *Polarons in Advanced Materials*, edited by A. S. Alexandrov (Springer-Verlag, Dordrecht, 2007).
[4] J. Tersoff and D. R. Hamann, Phys. Rev. B **31**, 805 (1985).
[5] A. Damascelli, Z. Hussain, and Z.-X. Shen, Rev. Mod. Phys. **75**, 473 (2003).
[6] N. Reyren *et al.*, Science **317**, 1196 (2007).
[7] M. Berciu, Phys. Rev. Lett. **97**, 036402 (2006); G. L. Goodvin, M. Berciu, and G. A. Sawatzky, Phys. Rev. B **74**, 245104 (2006); M. Berciu and G. L. Goodvin, Phys. Rev. B **76**, 165109 (2007).
[8] G. L. Goodvin and M. Berciu, Phys. Rev. B **78**, 235120 (2008); L. Covaci and M. Berciu, Europhys. Lett. **80**, 67 001 (2007); Phys. Rev. Lett. **100**, 256405 (2008).
[9] M. Berciu, A. S. Mishchenko, and N. Nagaosa, arXiv:0906.1233.
[10] N. V. Prokof'ev and B. V. Svistunov, Phys. Rev. Lett. **81**, 2514 (1998).
[11] Very recent work by R. Nourafkan, M. Capone, and N. Nafari, arXiv:0905.1379 [Phys. Rev. B (to be published)], focuses on very different aspects of this problem, for finite electron concentrations.
[12] T. L. Einstein and J. R. Schrieffer, Phys. Rev. B **7**, 3629 (1973).
[13] L. Covaci *et al.* (unpublished).
[14] I. Tamm, Phys. Z. Sowjetunion **1**, 733 (1932).
[15] This strong surface state is not seen if we set $v(j, \omega) = 0$, since here $U/t^* \approx 1.2$ only binds weakly a shallow state.